SUPPLEMENTAL INFORMATION

Figure S1. Retro-TRAP labeling of corticostriatal projection neurons, related to Figure 2.

Figure S2. WGCNA analysis of R6/2 model TRAP data, related to Figure 2.

Figure S3. Shared predicted regulators in cell types assessed in TRAP, related to Figures 2 and 3.

Figure S4. The Q170 and zQ175DN (zQ175) knockin models display similar gene expression changes in SPNs at 6-months of age, as reported by TRAP, related to Figure 3.

Figure S5. Differentially expressed genes in astroglia from the striatum of 6-month old CAG knockin allele model tissue, as reported by TRAP, related to Figure 3.

Figure S6. Comparison of dSPN and iSPN differentially expressed genes across the R6/2 and the zQ175DN models, as reported by TRAP, related to Figures 2 and 3.

Figure S7. WGCNA analysis of dSPN and iSPN 6-months of age allelic series TRAP data, related to Figure 3.

Figure S8. ACTIONet plots of all snRNA-Seq clustered cell types in mouse striatal tissue, with marked expression of known cell type marker genes, related to Figure 4.

Figure S9. Differentially expressed genes, as reported by snRNA-Seq, in additional cell types that were not shown in Figures 4 and 5, related to Figures 4 and 5.

Figure S10. Predicted regulators of dSPN and iSPN gene expression changes in the R6/2 and zQ175DN models, as reported by snRNA-Seq, related to Figure 4.

Figure S11. Comparison of TRAP and snRNA-Seq reported gene expression changes across models and SPN subtypes, related to Figures 2-4.

Figure S12. Contribution, by HD grade, of nuclei to the final HD cell type groups used for snRNA-Seq differential gene expression analysis, related to Figure 5.

Figure S13. Expression heatmaps of mtRNAs projected onto ACTIONet plot for human cell types, related to Figure 5.

Figure S14. Contribution of SPNs by HD grade and expression heatmaps of mtRNAs projected onto ACTIONet plots for SPNs, related to Figure 5.

Figure S15. Predicted top-ranked transcriptional regulators of perturbed genes across all cell types in the human HD snRNA-Seq data, and comparison of human HD snRNA-Seq data to GeM-HD study data, related to Figure 5.

Figure S16. Comparison of human HD snRNA-Seq data to the zQ175DN and R6/2 mouse model snRNA-Seq data, related to Figures 4 and 5.

Figure S17. WGCNA analysis of iSPN 3- and 6-months of age allelic series TRAP data, related to Figures 3, 5, and 7.

Figure S18. mHTT promotes the accumulation of cytosolic mtDNA, and striatal enrichment of TOMM70A related to Figure 7.

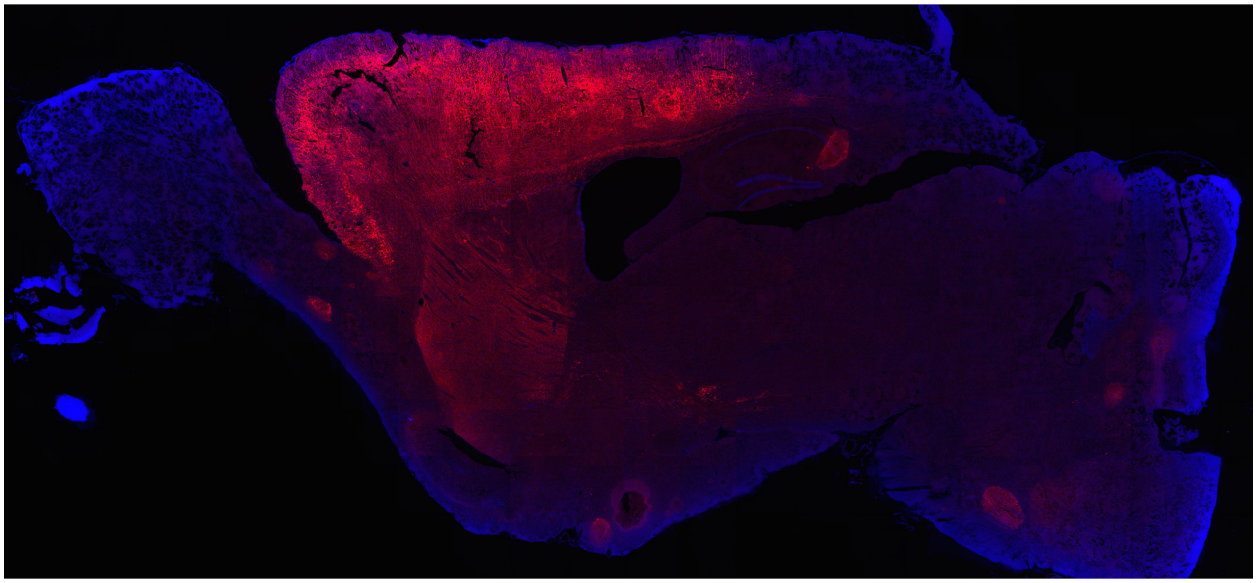

Figure S1. Retro-TRAP labeling of corticostriatal projection neurons, related to Figure 2. A tiled scan stack of a sagittal mouse brain section showing corticostriatal projection neurons (in red pseudocolor, note the labeled corticostriatal projection neuron axons extending into the striatum; neuropil, not cellular signal in the striatum) targeted by striatal injection of a Retro-TRAP virus (STAR Methods).

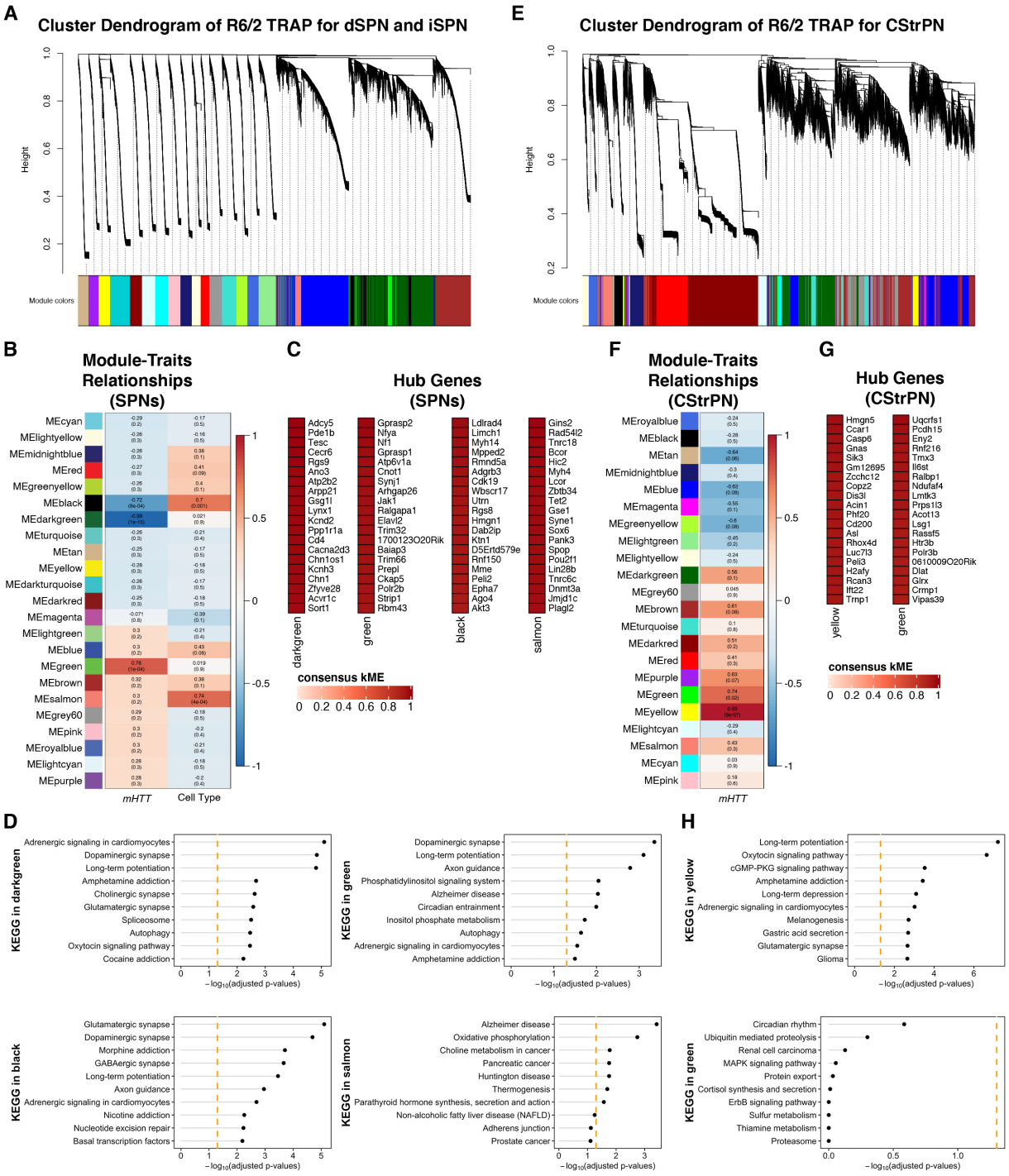
A
Cluster Dendrogram of R6/2 TRAP for dSPN and iSPN
Height
Module colors
E
Cluster Dendrogram of R6/2 TRAP for CStrPN
B
Module-Traits Relationships (SPNs)
MEcyan
MElightyellow
MEmidnightblue
MEred
MEgreenyellow
MEblack
MEdarkgreen
MEturquoise
MEtan
MEyellow
MEdarkturquoise
MEdarkred
MEmagenta
MElightgreen
MEblue
MEgreen
MEbrown
MEsalmon
MEgrey60
MEpink
MEroyalblue
MElightcyan
MEpurple
mHTT
Cell Type
C
Hub Genes (SPNs)
darkgreen
Adcy5 Pde1b Tesc Cecr6 Rgs9 Ano3 Atp2b2 Arpp21 Gsg1l Lynx1 Kcnd2 Ppp1r1a Cd4 Cacna2d3 Chn1os1 Kcnh3 Chn1 Zfyve28 Acvr1c Sort1
green
Gprasp2 Nfya Nf1 Gprasp1 Atp6v1a Cnot1 Synj1 Arhgap26 Jak1 Ralgapa1 Elavl2 Trim32 1700123O20Rik Baiap3 Trim66 Prepl Ckap5 Polr2b Strip1 Rbm43
black
Ldlrad4 Limch1 Myh14 Mpped2 Rmnd5a Adgrb3 Cdk19 Wbscr17 Utrn Rgs8 Hmgn1 Dab2ip Ktn1 D5Ertd579e Rnf150 Mme Peli2 Epha7 Ago4 Akt3
salmon
Gins2 Rad54l2 Tnrc18 Bcor Hic2 Myh4 Lcor Zbtb34 Tet2 Gse1 Syne1 Sox6 Pank3 Spop Pou2f1 Lin28b Tnrc6c Dnmt3a Jmjd1c Plagl2
consensus kME
0 0.2 0.4 0.6 0.8 1
F
Module-Traits Relationships (CStrPN)
MEroyalblue
MEblack
MEtan
MEmidnightblue
MEblue
MEmagenta
MEgreenyellow
MElightgreen
MElightyellow
MEdarkgreen
MEgrey60
MEbrown
MEturquoise
MEdarkred
MEred
MEpurple
MEgreen
MEyellow
MElightcyan
MEsalmon
MEcyan
MEpink
mHTT
G
Hub Genes (CStrPN)
yellow
Hmgn5 Ccar1 Casp6 Gnas Slk3 Gm12695 Zcchc12 Copz2 Dis3l Acin1 Phf20 Cd200 Asl Rhox4d Luc7l3 Peli3 H2afy Rcan3 Ift22 Trnp1
green
Uqcrfs1 Pcdh15 Eny2 Rnf216 Tmx3 Il6st Ralbp1 Ndufaf4 Lmtk3 Prps1l3 Acot13 Lsg1 Rassf5 Htr3b Polr3b 0610009O20Rik Dlat Glrx Crmp1 Vipas39
consensus kME
0 0.2 0.4 0.6 0.8 1
D
KEGG in darkgreen
Adrenergic signaling in cardiomyocytes
Dopaminergic synapse
Long-term potentiation
Amphetamine addiction
Cholinergic synapse
Glutamatergic synapse
Spliceosome
Autophagy
Oxytocin signaling pathway
Cocaine addiction
KEGG in green
Dopaminergic synapse
Long-term potentiation
Axon guidance
Phosphatidylinositol signaling system
Alzheimer disease
Circadian entrainment
Inositol phosphate metabolism
Autophagy
Adrenergic signaling in cardiomyocytes
Amphetamine addiction
KEGG in black
Glutamatergic synapse
Dopaminergic synapse
Morphine addiction
GABAergic synapse
Long-term potentiation
Axon guidance
Adrenergic signaling in cardiomyocytes
Nicotine addiction
Nucleotide excision repair
Basal transcription factors
KEGG in salmon
Alzheimer disease
Oxidative phosphorylation
Choline metabolism in cancer
Pancreatic cancer
Huntington disease
Thermogenesis
Parathyroid hormone synthesis, secretion and action
Non-alcoholic fatty liver disease (NAFLD)
Adherens junction
Prostate cancer
H
KEGG in yellow
Long-term potentiation
Oxytocin signaling pathway
cGMP-PKG signaling pathway
Amphetamine addiction
Long-term depression
Adrenergic signaling in cardiomyocytes
Melanogenesis
Gastric acid secretion
Glutamatergic synapse
Glioma
KEGG in green
Circadian rhythm
Ubiquitin mediated proteolysis
Renal cell carcinoma
MAPK signaling pathway
Protein export
Cortisol synthesis and secretion
ErbB signaling pathway
Sulfur metabolism
Thiamine metabolism
Proteasome
−log10(adjusted p-values)

Figure S2. WGCNA analysis of R6/2 model TRAP data, related to Figure 2. Consensus coexpression network analysis of the dSPN and iSPN R6/2 TRAP data reveals multiple *mHTT*-and SPN cell type-associated modules, each labeled by a unique color in the clustering dendrogram (**A**) and in the module-trait table that represents the Pearson correlation of each module eigengene with the specified trait (either the presence of *mHTT* or Cell Type) (**B**). Also shown are the top module hub genes (**C**) and the top ten KEGG enriched pathways (**D**) in selected modules from **B**. Similar consensus coexpression network analysis of the CStrPN R6/2 TRAP data, revealing top *mHTT*-associated modules in the clustering dendrogram (**E**) and module-trait table (**F**), as well as the top module hub genes (**G**) and the top ten KEGG enriched pathways (**H**) in selected modules from **F**. **B and F:** red signifies a strong positive correlation and blue signifies a strong negative correlation, and Fisher's asymptotic test *p*-values for the module-trait relationships are listed below each correlation. **C and G:** Hub genes in each consensus module were those defined as having expression values that were highly correlated with that module's eigengene values (consensus kME). **D and H:** KEGG pathway analysis results are represented with Fisher's exact test $-\log_{10}$-adjusted *p*-value and the yellow dashed line notes the significance threshold.

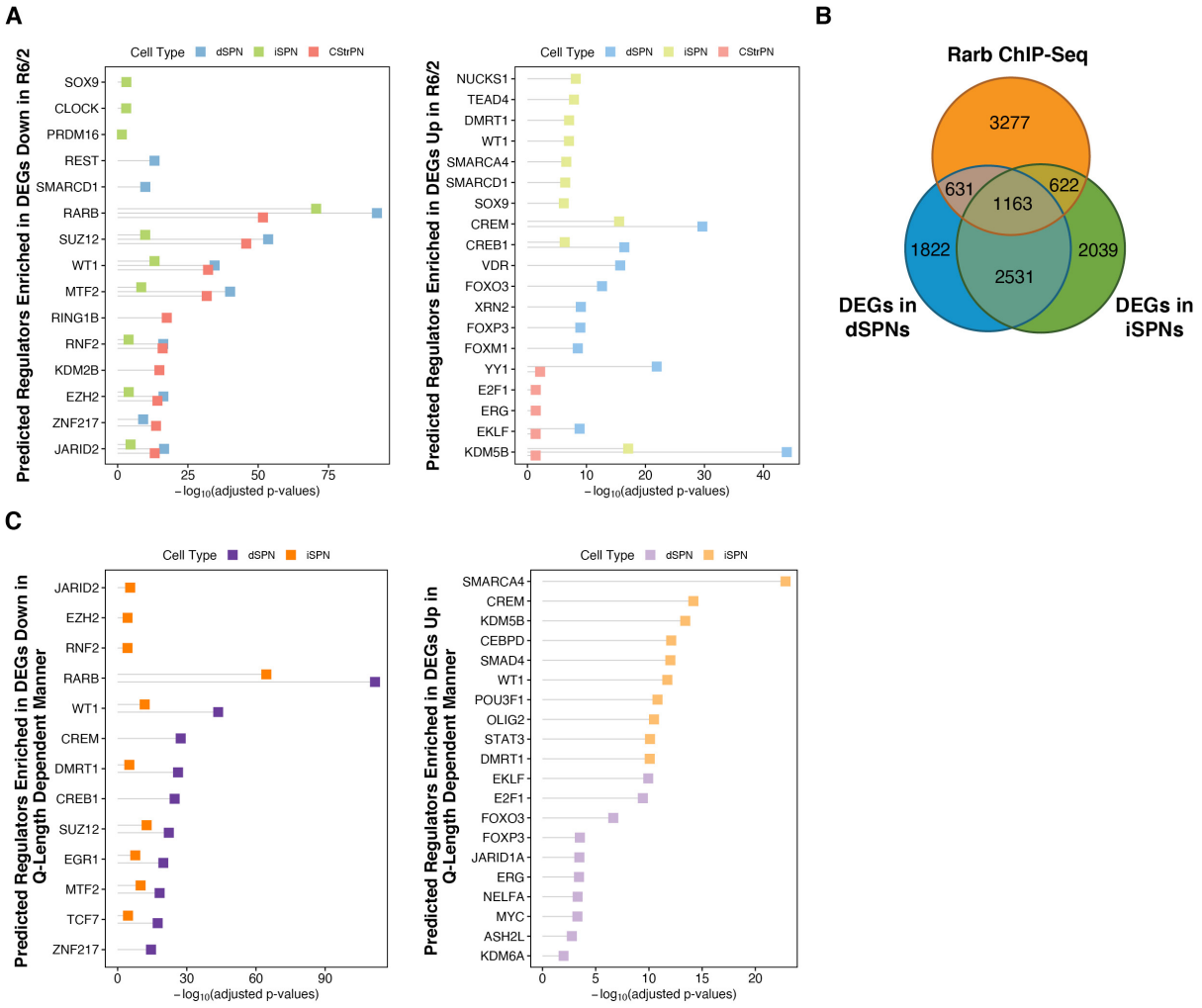

Figure S3. Shared predicted regulators in cell types assessed in TRAP, related to Figures 2 and 3. (A) Predicted transcriptional regulators, by ChEA analysis, of genes that were downregulated (left panel) and upregulated (right panel) across the three cell types profiled in the R6/2 model, represented with Fisher's exact test $-\log_{10}$-adjusted *p*-value. **(B)** Venn overlap analysis of overlap between published striatal Rarb ChIP-Seq data, as well as genes dysregulated in either dSPNs or iSPNs in the R6/2 model. **(C)** Geneset enrichment analysis using ChEA annotations to predict transcriptional regulators of genes that were downregulated (left panel) and upregulated (right panel) across dSPNs and iSPNs in a CAG-length dependent manner in the full-length *mHTT* knockin models, represented with Fisher's exact test $-\log_{10}$-adjusted *p*-value.

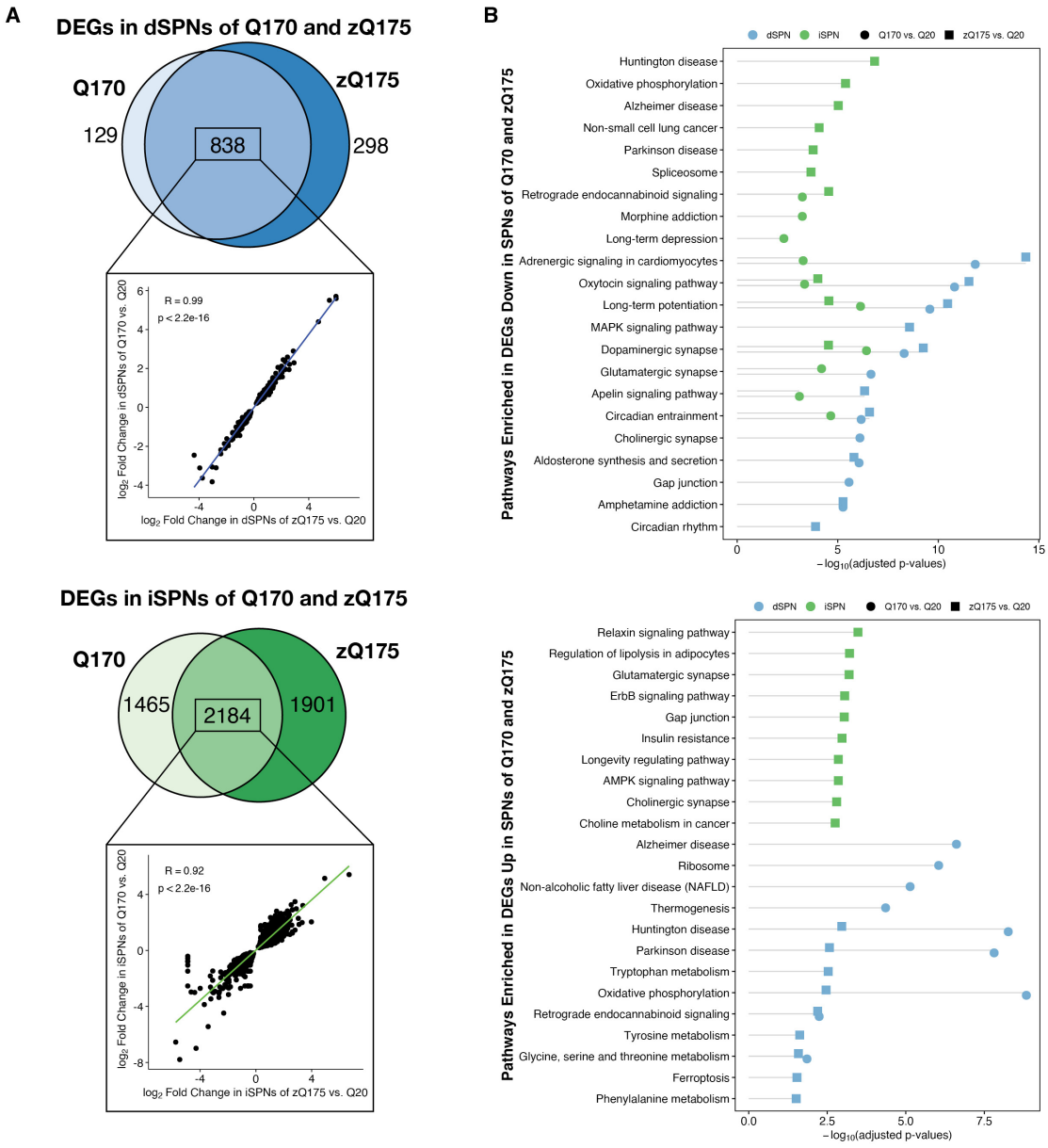

Figure S4. The Q170 and zQ175DN (zQ175) knockin models display similar gene expression changes in SPNs at 6-months of age, as reported by TRAP, related to Figure 3. **(A)** Venn diagram overlap analysis of differentially expressed genes in dSPNs (top panel) and iSPNs (bottom panel) of the Q170 and zQ175DN knockin models (each compared to Q20 control). A high degree of overlap was observed in dSPNs, and to a lesser extent, iSPNs. **(B)** KEGG pathway analysis of genes downregulated (top panel) and upregulated (bottom panel) in dSPNs and iSPNs of the Q170 and zQ175DN knockin models (each compared to Q20 control), represented with Fisher's exact test $-\log_{10}$-adjusted *p*-value.

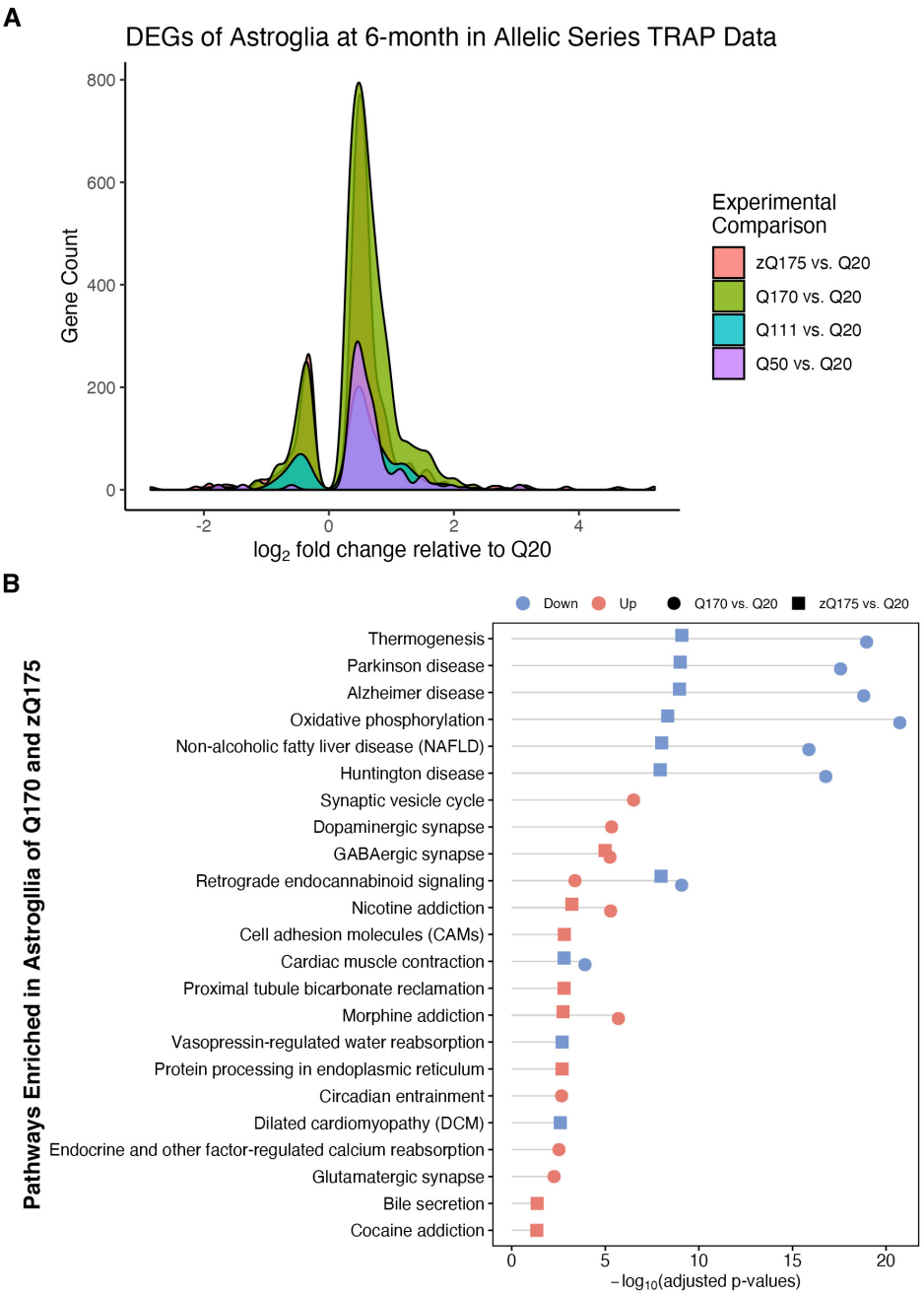

Figure S5. Differentially expressed genes in astroglia from the striatum of 6-month old CAG knockin allele model tissue, as reported by TRAP, related to Figure 3.

(A) Number of differentially expressed genes for each knockin allele studied in the astroglial study (each comparison vs. Q20). **(B)** KEGG pathway analysis of genes downregulated and upregulated in astroglia of the Q170 and zQ175DN knockin models (each compared to Q20 control), represented with Fisher's exact test $-\log_{10}$-adjusted *p*-value.

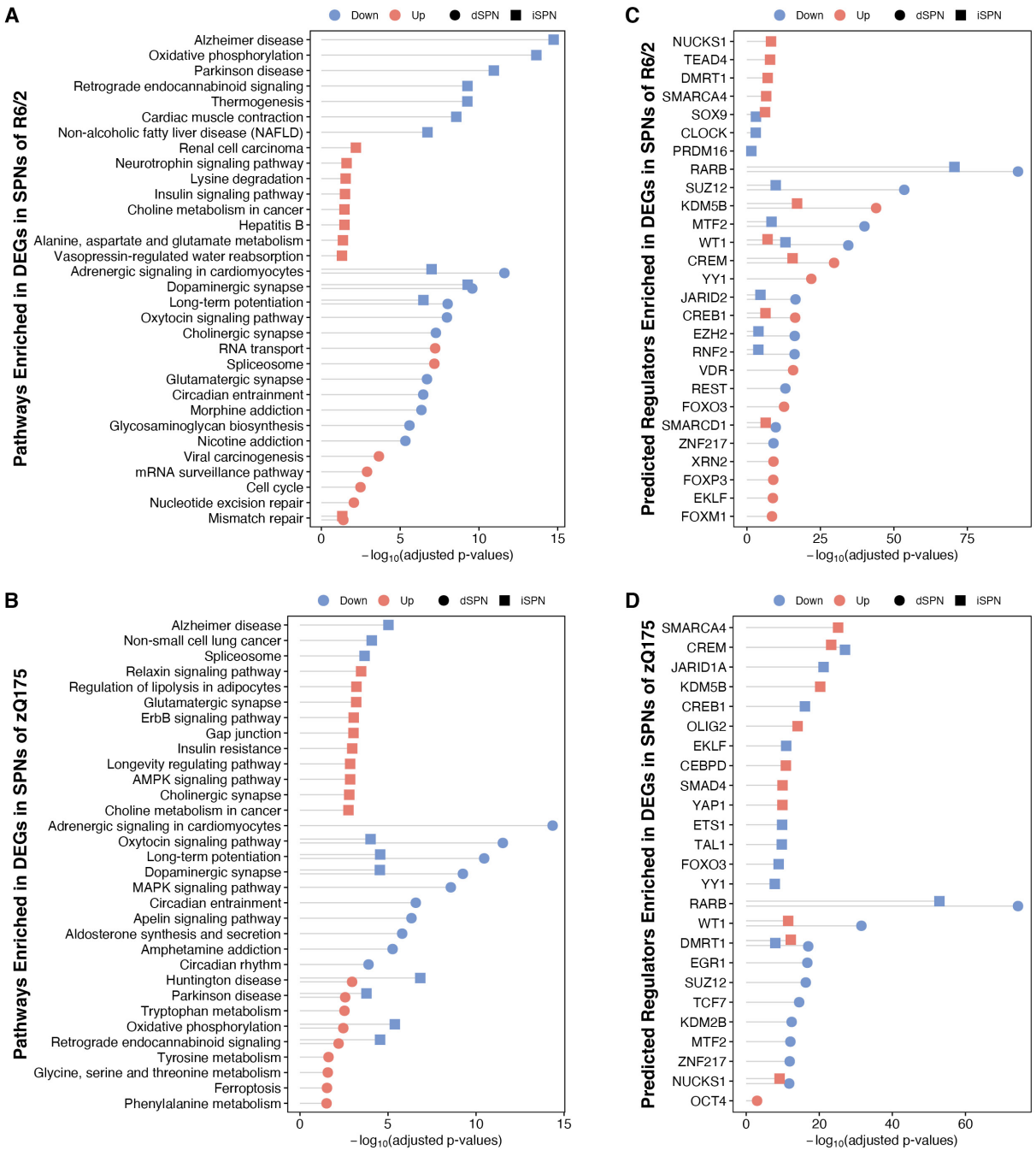

Figure S6. Comparison of dSPN and iSPN differentially expressed genes across the R6/2 and the zQ175DN models, as reported by TRAP, related to Figures 2 and 3.

KEGG pathway analysis (**A, B**) and predicted regulators (**C, D**) of genes downregulated and upregulated in dSPNs and iSPNs of the R6/2 and zQ175DN knockin models, represented with Fisher's exact test $-\log_{10}$-adjusted *p*-value.

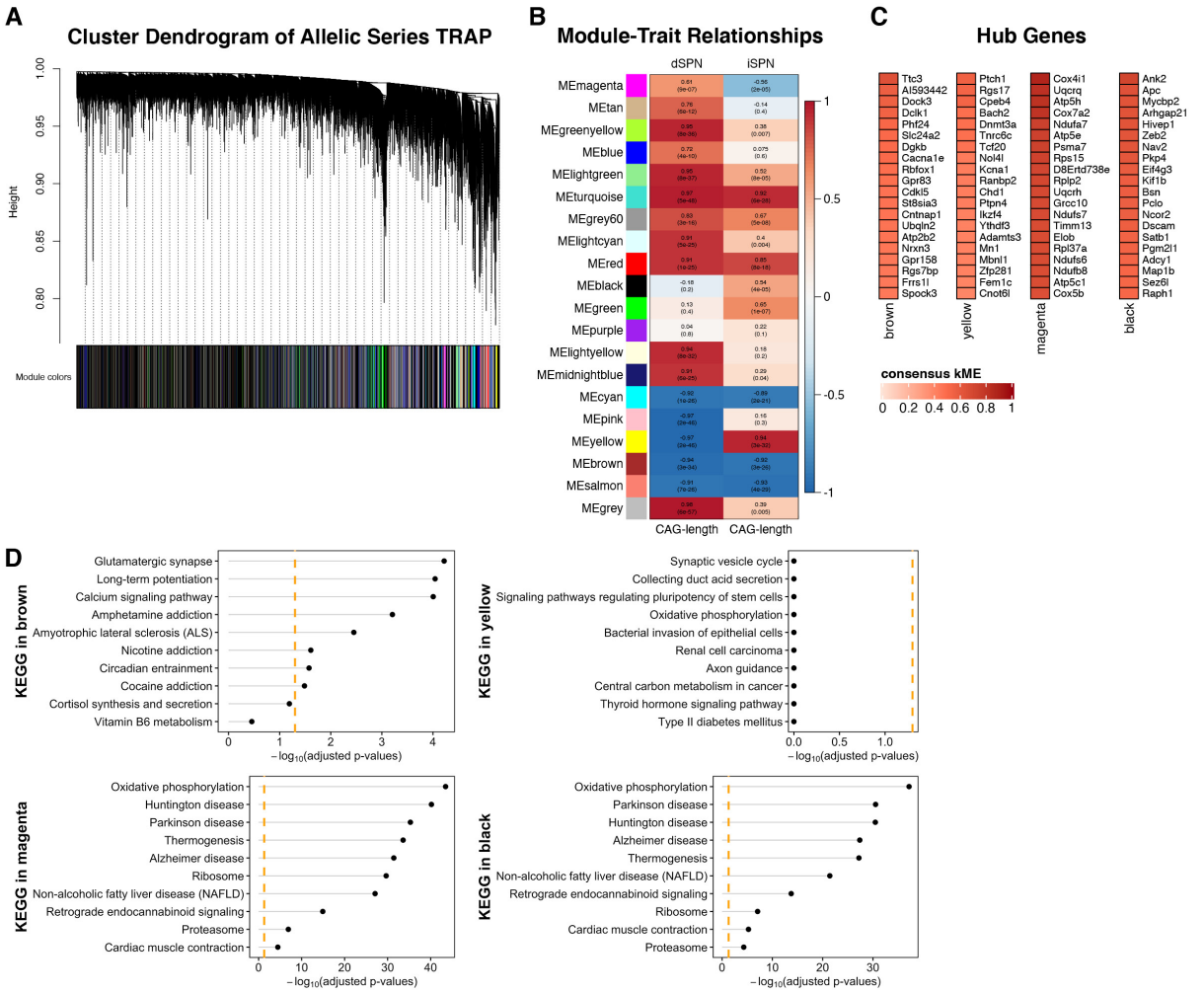

Figure S7. WGCNA analysis of dSPN and iSPN 6-months of age allelic series TRAP data, related to Figure 3. Consensus coexpression network analysis of the dSPN and iSPN 6-months of age allelic series TRAP data reveals multiple CAG-length-associated modules, each labeled by a unique color in the clustering dendrogram (**A**) and in the module-trait table that represents the Pearson correlation of each module eigengene with CAG-length (**B**). Also shown are the top module hub genes (**C**) and the top ten KEGG enriched pathways (**D**) in selected modules from **B**. **B:** red signifies a strong positive correlation and blue signifies a strong negative correlation, and Fisher's asymptotic test *p*-values for the module-trait relationships are listed below each correlation. **C:** Hub genes in each consensus module were those defined as having expression values that were highly correlated with that module's eigengene values (consensus kME). **D:** KEGG pathway analysis results are represented with Fisher's exact test $-\log_{10}$-adjusted *p*-value and the yellow dashed line notes the significance threshold.

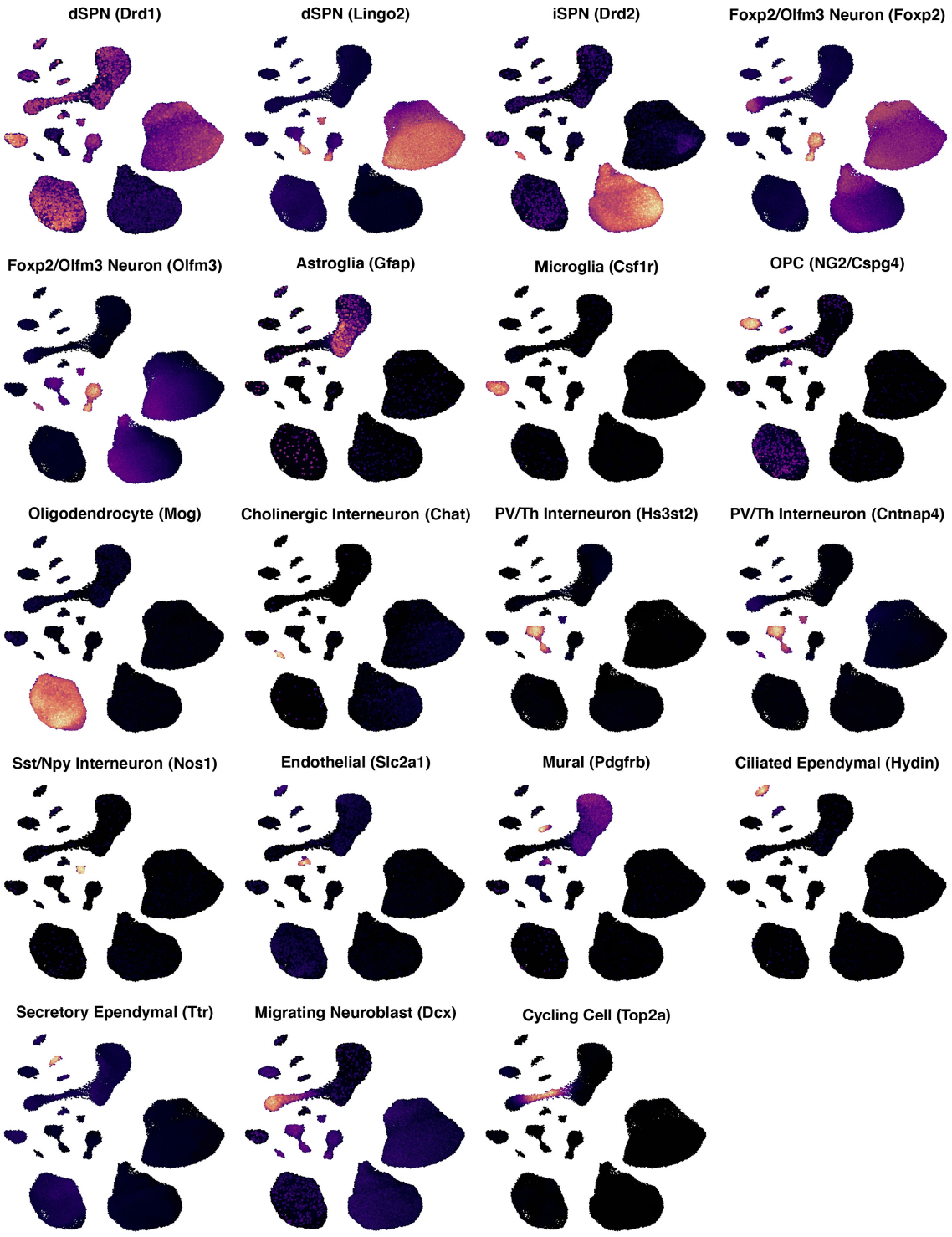

Figure S8. ACTIONet plots of all snRNA-Seq clustered cell types in mouse striatal tissue, with marked expression of known cell type marker genes, related to Figure 4. From the control and R6/2 model groups, same cluster identities as in Figure 4A.

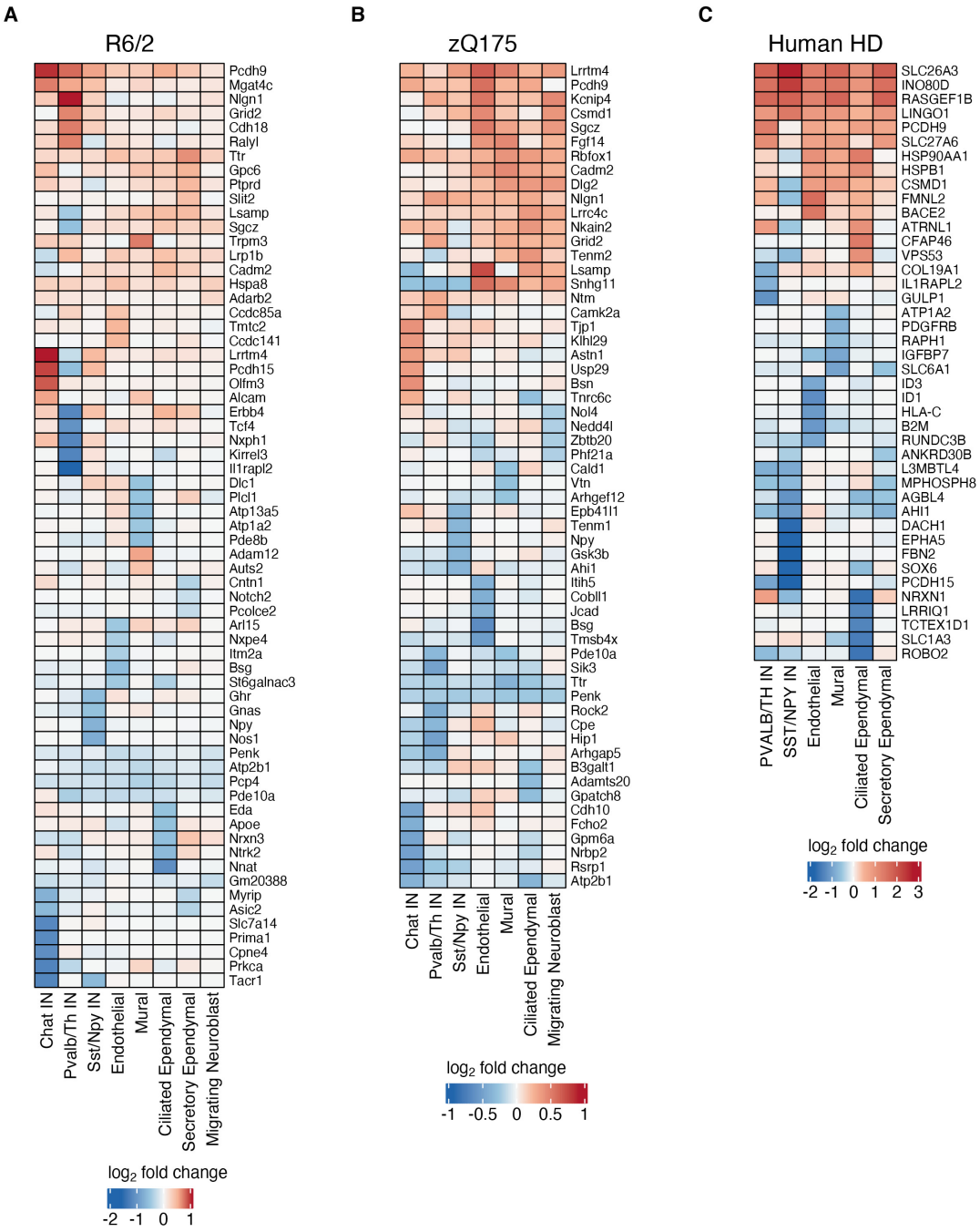

Figure S9. Differentially expressed genes, as reported by snRNA-Seq, in additional cell types that were not shown in Figures 4 and 5, related to Figures 4 and 5. Expression heatmaps of the top five most downregulated and upregulated protein-coding genes by $\log_2$-fold change in less abundant cell types from the R6/2 **(A)**, zQ175DN **(B)**, and human HD **(C)** snRNA-Seq datasets. Genes were selected by $\log_2$-fold change only, with no *p*-value cutoff applied.

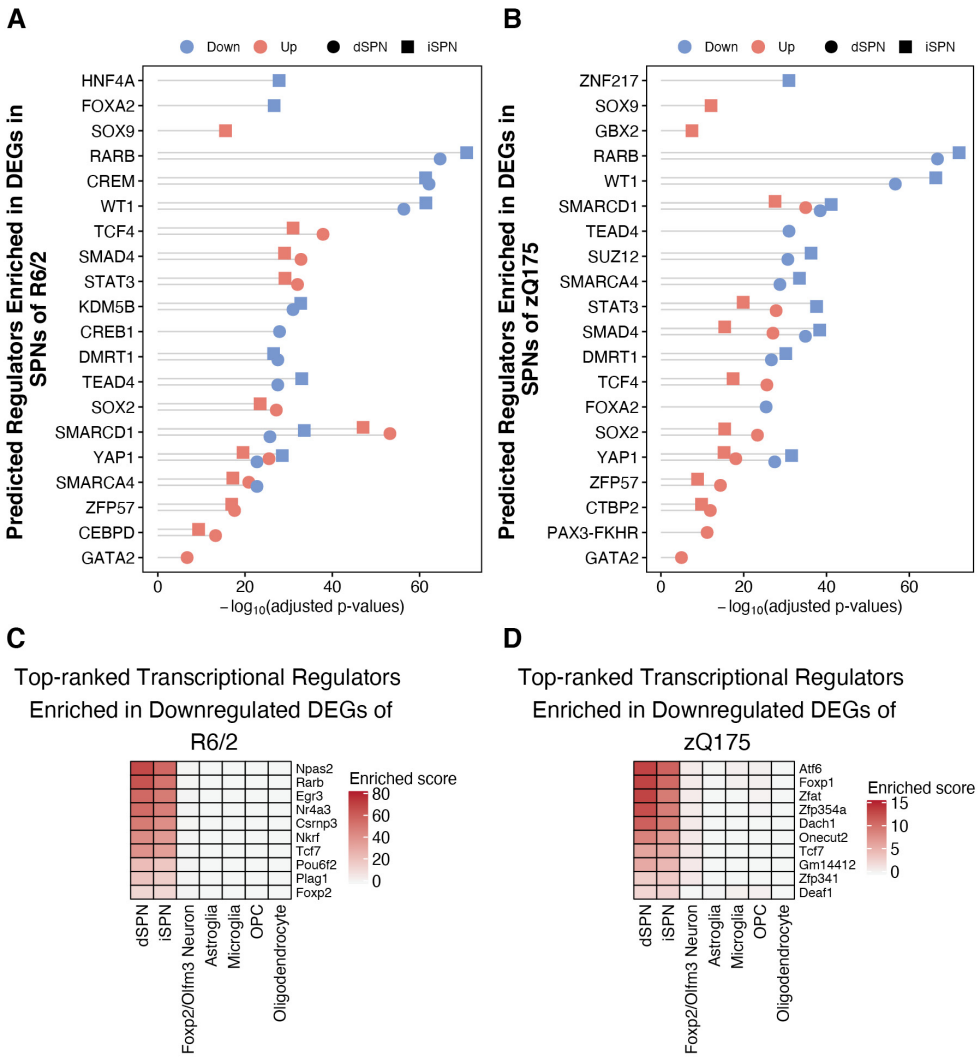

Figure S10. Predicted regulators of dSPN and iSPN gene expression changes in the R6/2 and zQ175DN models, as reported by snRNA-Seq, related to Figure 4. (A-B) Comparison of dSPN and iSPN differentially expressed gene predicted regulators across the R6/2 **(A)** and zQ175DN **(B)** models as predicted by Chromatin Enrichment Analysis of the snRNA-Seq data. Predicted top-ranked transcriptional regulators of downregulated genes in R6/2 **(C)** and in zQ175DN **(D)** estimated using the ACTIONet framework based on the meta-analysis of the activity of their downstream targets (additional cell types here shown for comparison). Reported values are the -$\log_{10}$ of meta-*p*-values. This ACTIONet framework analysis is only shown for the downregulated genes, as there were no significantly ranked predicted transcriptional regulators for the upregulated genes.

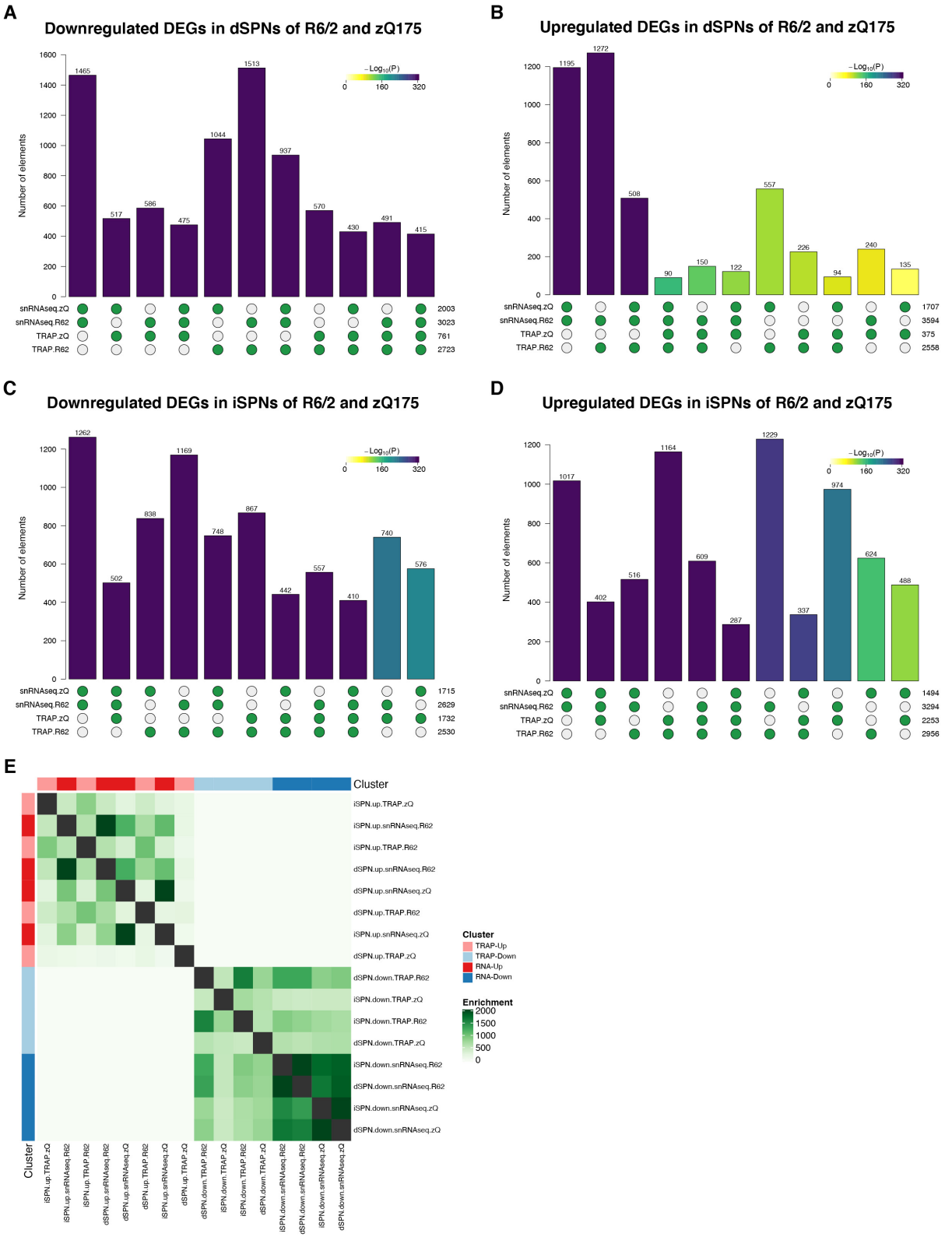
A
Downregulated DEGs in dSPNs of R6/2 and zQ175
Number of elements
−Log10(P)
0
160
320
1465
517
586
475
1044
1513
937
570
430
491
415
snRNAseq.zQ
snRNAseq.R62
TRAP.zQ
TRAP.R62
2003
3023
761
2723
B
Upregulated DEGs in dSPNs of R6/2 and zQ175
1195
1272
508
90
150
122
557
226
94
240
135
1707
3594
375
2558
C
Downregulated DEGs in iSPNs of R6/2 and zQ175
1262
502
838
1169
748
867
442
557
410
740
576
1715
2629
1732
2530
D
Upregulated DEGs in iSPNs of R6/2 and zQ175
1017
402
516
1164
609
287
1229
337
974
624
488
1494
3294
2253
2956
E
Cluster
iSPN.up.TRAP.zQ
iSPN.up.snRNAseq.R62
iSPN.up.TRAP.R62
dSPN.up.snRNAseq.R62
dSPN.up.snRNAseq.zQ
dSPN.up.TRAP.R62
iSPN.up.snRNAseq.zQ
dSPN.up.TRAP.zQ
dSPN.down.TRAP.R62
iSPN.down.TRAP.zQ
iSPN.down.TRAP.R62
dSPN.down.TRAP.zQ
iSPN.down.snRNAseq.R62
dSPN.down.snRNAseq.R62
iSPN.down.snRNAseq.zQ
dSPN.down.snRNAseq.zQ
Cluster
TRAP-Up
TRAP-Down
RNA-Up
RNA-Down
Enrichment
2000
1500
1000
500
0

Figure S11. Comparison of TRAP and snRNA-Seq reported gene expression changes across models and SPN subtypes, related to Figures 2-4. Differentially expressed genes from the snRNA-Seq and TRAP studies were identified using a one-sided Welch *t*-test or a negative binomial model test (DESeq2), respectively (STAR Methods). Each mouse model/technology platform combination was independently thresholded to identify a set of perturbed upregulated and downregulated genes. Finally, a statistical test of multi-set intersections between perturbed genes was performed using the SuperExactTest (Wang et al., 2015) and reported for dSPN (**A**) downregulated genes, and (**B**) upregulated genes, as well as iSPN (**C**) downregulated genes, and (**D**) upregulated genes. A-D: The number above each bar represents the overlap in genes per comparison. Below each bar, green circles indicate the gene sets that were considered in each comparison, and numbers to the right indicate the total size of each of these individual gene sets. Bars are colored according to their statistical significance as noted in the insert. Panel **E** provides an alternative view in which pairwise set overlaps are computed, individually, to construct a similarity graph. An adjacency matrix heatmap is shown while gene-set groups (4 clusters) with similar behavior are marked.

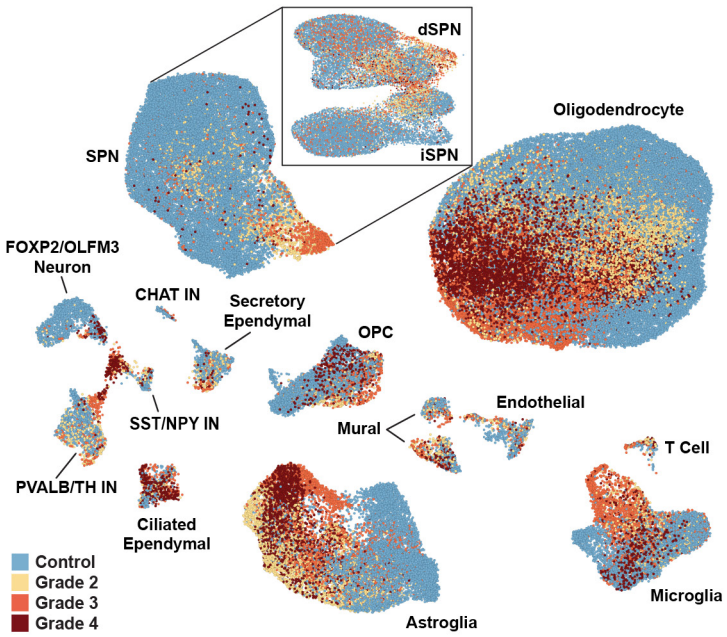

Figure S12. Contribution, by HD grade, of nuclei to the final HD cell type groups used for snRNA-Seq differential gene expression analysis, related to Figure 5. ACTIONet plots graphically demonstrating the contribution of each HD grade to each cell type identified in the pooled analysis HD human tissue samples that were used for calling differentially expressed genes. Table S2 provides numbers in addition to this graphical demonstration.

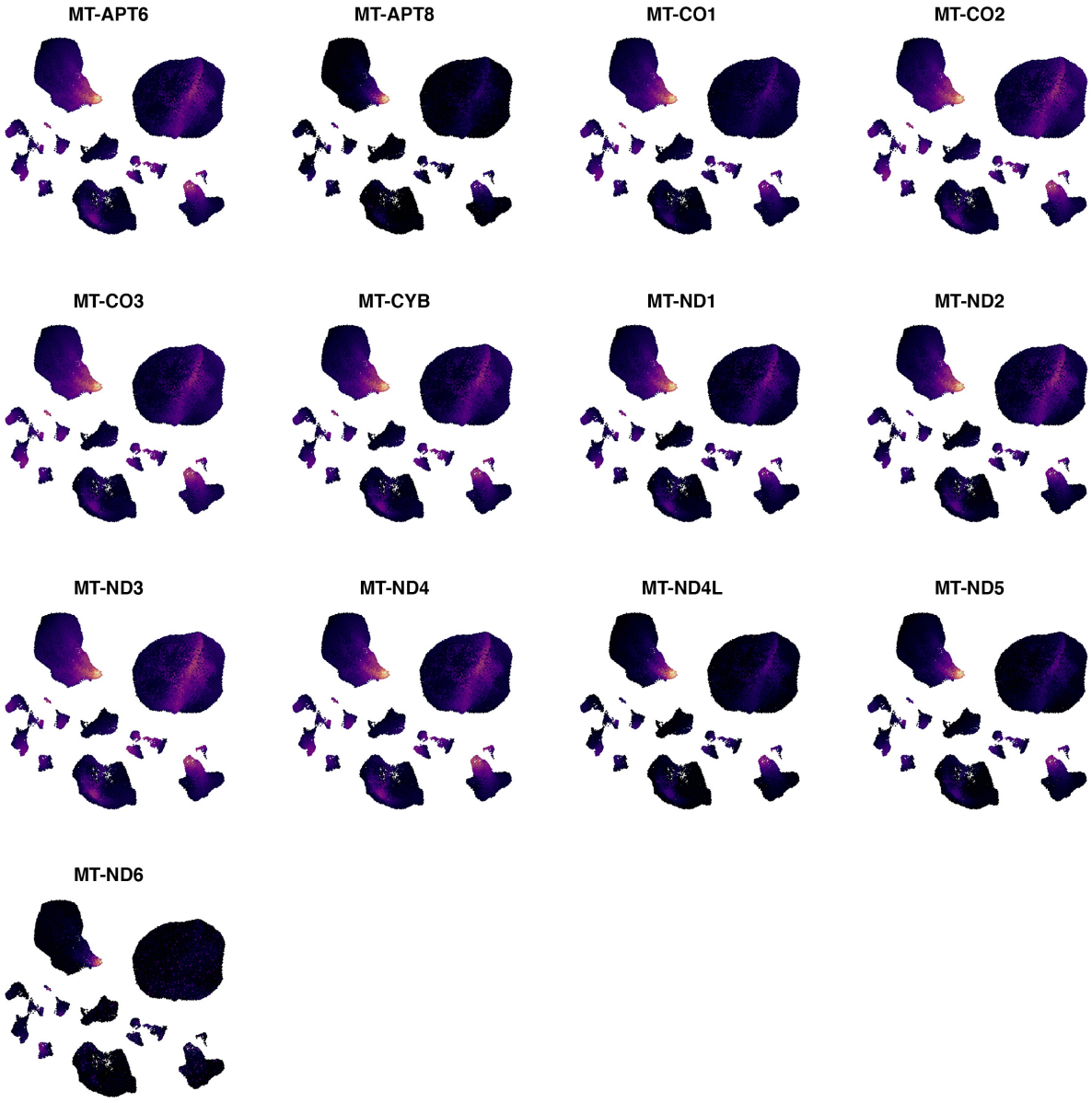

Figure S13. Expression heatmaps of mtRNAs projected onto ACTIONet plot for human cell types, related to Figure 5. mtRNA expression in HD caudate and putamen samples (same cluster identities as in Figures 5 and S12).

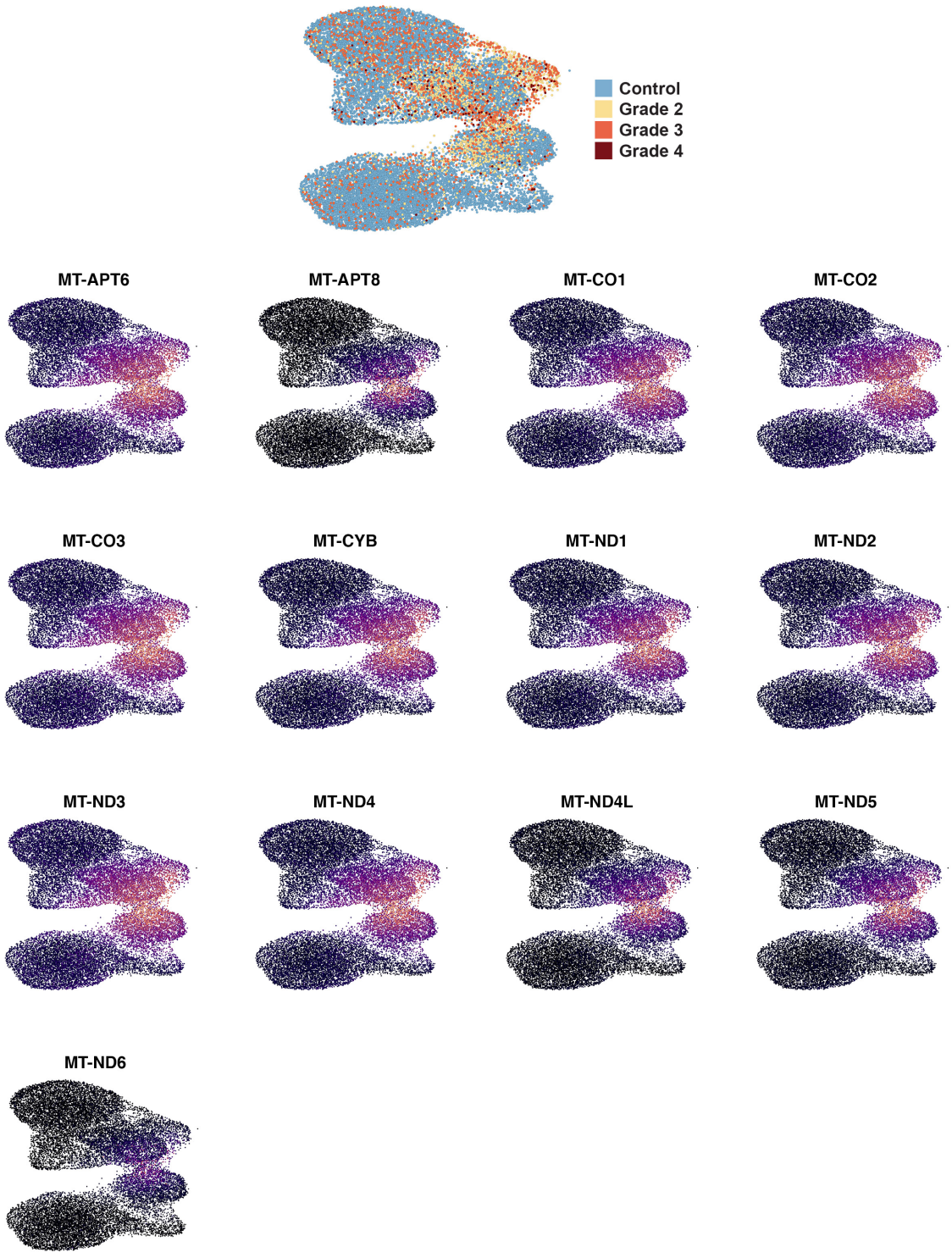

Figure S14. Contribution of SPNs by HD grade and expression heatmaps of mtRNAs projected onto ACTIONet plots for SPNs, related to Figure 5.

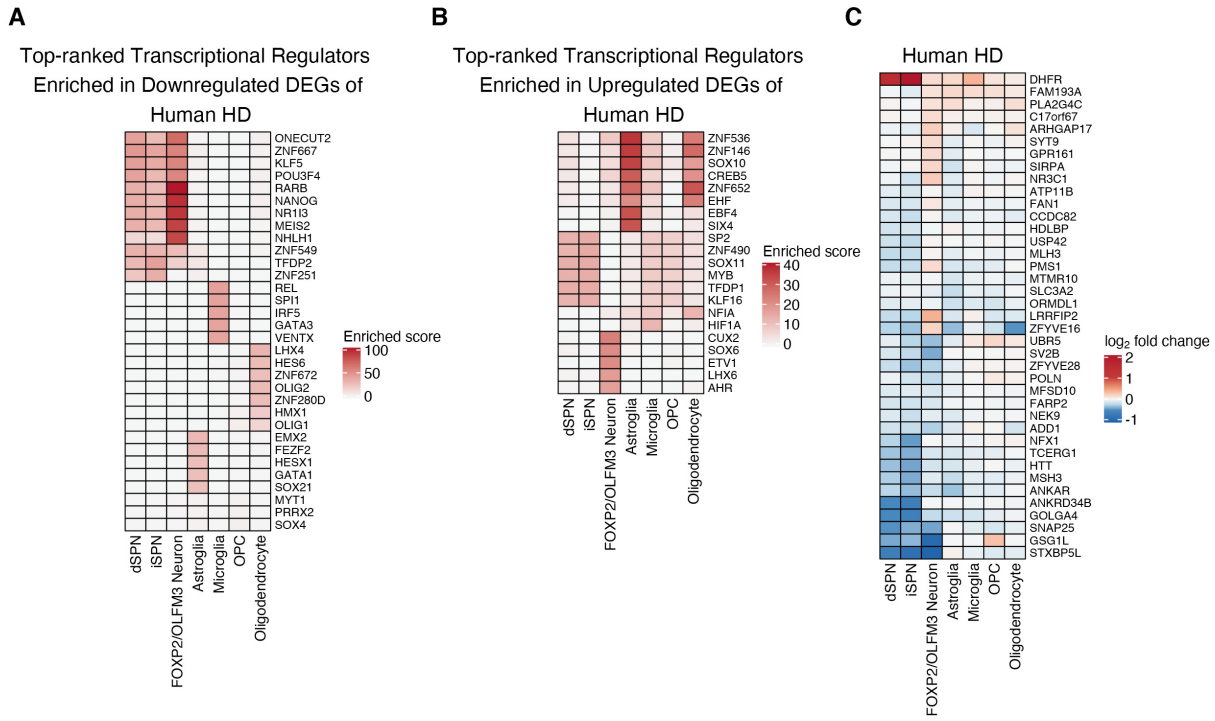

Figure S15. Predicted top-ranked transcriptional regulators of perturbed genes across all cell types in the human HD snRNA-Seq data and comparison of human HD snRNA-Seq data to GeM-HD study data, related to Figure 5. Predicted top-ranked transcriptional regulators of downregulated **(A)** and upregulated **(B)** genes in the human HD snRNA-Seq data, estimated using meta-analysis of the activity of their downstream targets [STAR Methods, (Keenan et al., 2019)]. Reported values are the -$\log_{10}$ of meta-*p*-values. **(C)** Reported values are $\log_2$-fold change of the overlapped genes between the GeM-HD GWAS modifiers with pGWA12345-3510 < 0.0005 and the DEGs in the human HD snRNA-Seq data.

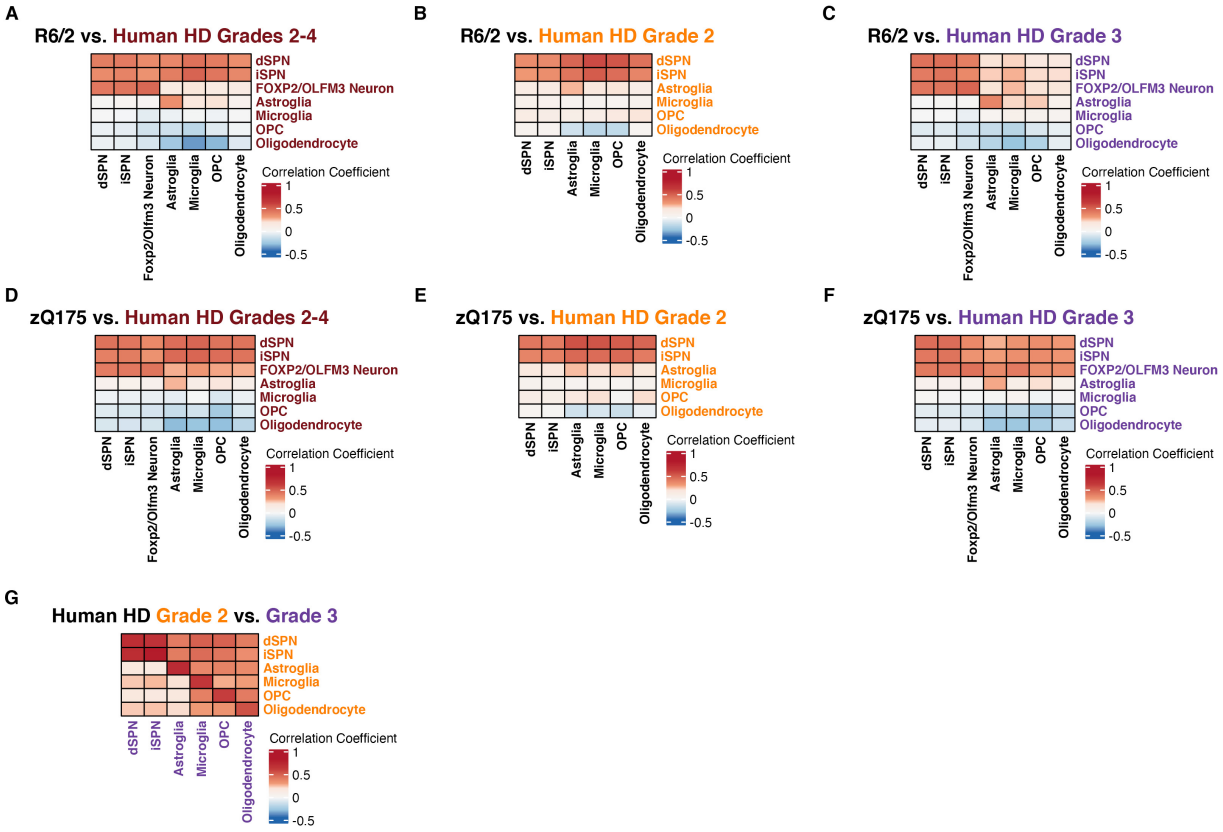

Figure S16. Comparison of human HD snRNA-Seq data to the zQ175DN and R6/2 mouse model snRNA-Seq data, related to Figures 4 and 5. Differentially expressed $\log_2$-fold-change of genes in case-vs.-control comparisons were computed and used as a quantitative measure of gene perturbation in each cell type/model. Values were batch-corrected and Pearson's correlation between profiles are reported for the comparisons between the human snRNA-Seq data and the R6/2 (**A-C**) and zQ175DN (**D-F**) model snRNA-Seq data by all HD grade (**A+D**), HD grade 2 only (**B+E**), or HD grade 3 only (**C+F**) comparisons. As a comparison, grade 2 HD human vs. grade 3 HD human snRNA-Seq data were highly correlated for all cell types (**G**).

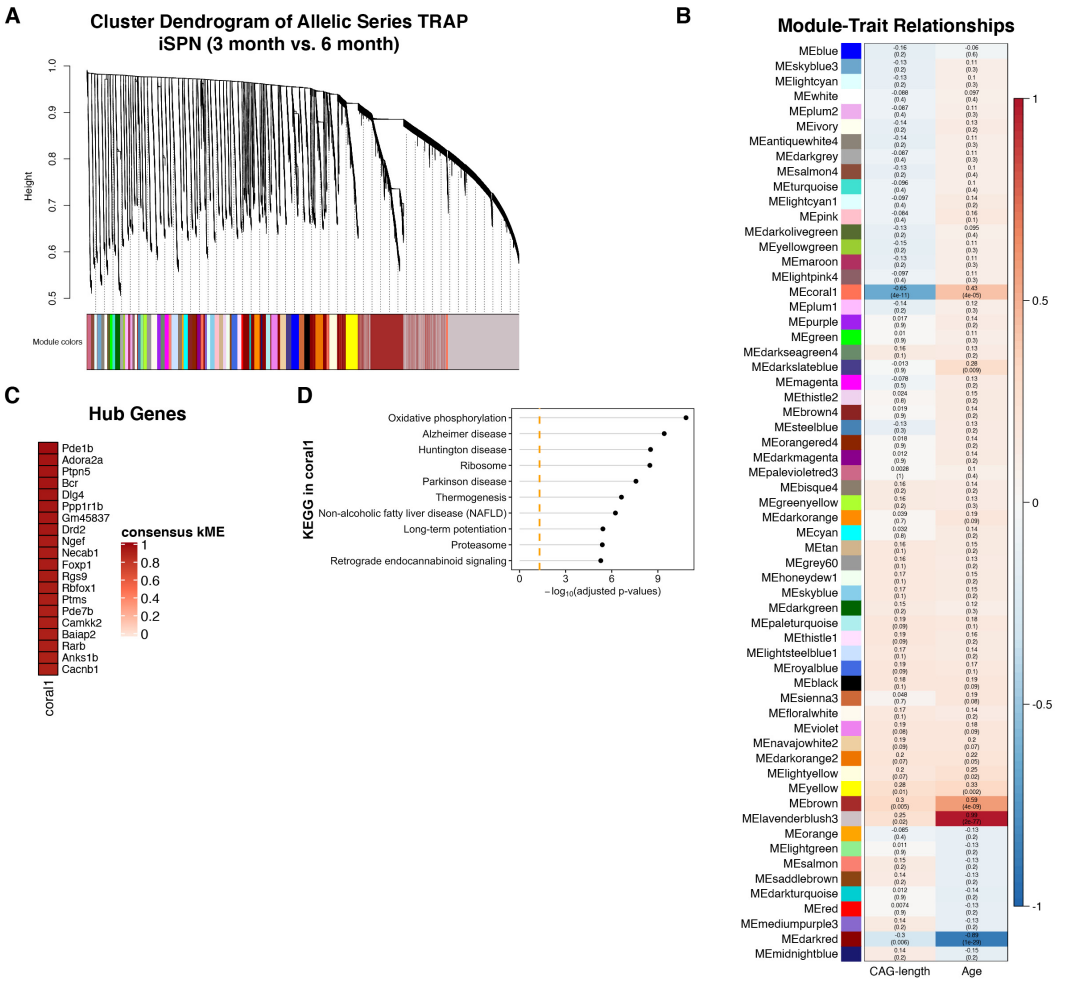

Figure S17. WGCNA analysis of iSPN 3- and 6-months of age allelic series TRAP data, related to Figures 3, 5, and 7. Consensus coexpression network analysis of the iSPN 3- and 6-months of age allelic series TRAP data reveals multiple CAG-length- and age-associated modules, each labeled by a unique color in the clustering dendrogram (**A**) and in the module-trait correlation table that represents the Pearson correlation of the module eigengene with the specified trait (CAG-length or Age) (**B**). Also shown are the top module hub genes (**C**) and the top ten KEGG enriched pathways (**D**) in selected modules from **B**. **B:** red signifies a strong positive correlation and blue signifies a strong negative correlation, and Fisher's asymptotic test *p*-values for the module-trait relationships are listed below each correlation. **C:** Hub genes in each consensus module were those defined as having expression values that were highly correlated with that module's eigengene values (consensus kME). **D:** KEGG pathway analysis results are represented with Fisher's exact test $-\log_{10}$-adjusted *p*-value and the yellow dashed line notes the significance threshold.

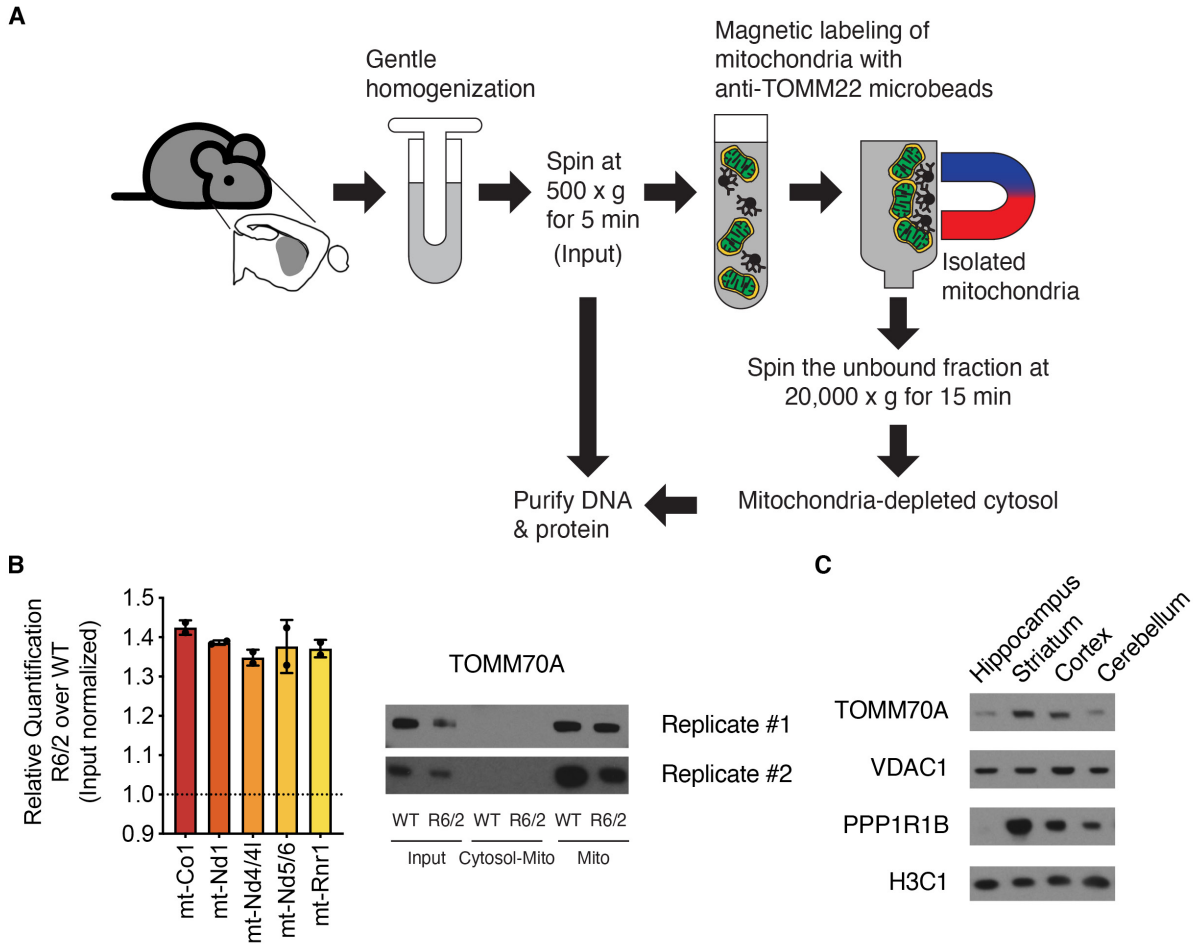

Figure S18. mHTT promotes the accumulation of cytosolic mtDNA, and striatal enrichment of TOMM70A related to Figure 7. (A) Schematic of the subcellular fractionation approach: after gentle dounce homogenization and clearing of unbroken cells by centrifugation for 5 min at 500 x *g* (input fraction), mitochondria are gently removed from the input fraction by immunomagnetic purification using anti-TOMM22 antibody-coated magnetic beads (which are then collected as the 'bound' mitochondrial fraction). The flow-through 'unbound' fraction was further depleted of any residual mitochondria with a second fractionation step, by centrifugation at 20, 000 x *g* for 15 min. The resulting supernatant from this centrifugation was the "cytosol - mitochondria" fraction used for studies presented in panel B. **(B)** Left panel: qPCR analysis of the "cytosol –mitochondria" fractions of R6/2 and isogenic control mouse striatal tissue revealed an increase in cytosolic mtDNA content for DNAs encoding mt-Co1, mt-Nd1, mt-Nd4, mt-Nd5,

and mt-Rnr1 in R6/2 as compared to isogenic control mice. Right panel: Western blot analysis of TOMM70A distribution in the subcellular fractionation samples revealed the presence of this mitochondrial marker only in the input and mitochondrial fractions, but not in the "cytosol - mitochondria fraction." (**C)** Western blot analysis of TOMM70A (the mouse ortholog of human TOMM70) expression across the indicated mouse brain regions, demonstrating that TOMM70A displays an expression pattern similar to the striatal-enriched protein DARPP-32 (PPP1R1B). VDAC is a control mitochondrial protein loaded for comparison, and histone protein H3C1 is a loading control.

REFERENCES

Keenan, A.B., Torre, D., Lachmann, A., Leong, A.K., Wojciechowicz, M.L., Utti, V., Jagodnik, K.M., Kropiwnicki, E., Wang, Z., and Ma'ayan, A. (2019). ChEA3: transcription factor enrichment analysis by orthogonal omics integration. Nucleic acids research *47*, W212-W224.

Wang, M., Zhao, Y., and Zhang, B. (2015). Efficient Test and Visualization of Multi-Set Intersections. Scientific reports *5*, 16923.